Chapter 1

Introduction

1.1 Reaction Dynamics

The aim of chemical reaction dynamics is to expand the understanding of the nature of uni- and bimolecular reactions, different kinds of energy transfer processes within and between atoms and molecules and elementary chemical processes such as photodissociation and photoionisation.[1] It is desirable to obtain a set of 'rules' that explain the outcome of simple reactions, and thus make it possible to predict the outcome of related or more complex reactions.[2] Even though chemical reactions are all constrained by the conservation of total energy and angular momentum, a variety of very different reaction mechanisms has been observed. The forces that act on the atoms and molecules involved in a reaction can be described by potential energy surfaces (PES) which represent the energy of a system with respect to all internal degrees of freedom.[3] Potential energy surfaces vary in shape, relative height(s) of the reaction barrier(s) and complexity and hence give rise to many different classes of chemical reactions.

A common way to gain insight into the mechanism of a simple reaction is to measure the internal and translational energy distribution of the nascent products.[4] Molecular beam experiments typically utilise time-of-flight detection methods yielding speed and angular distributions of all reaction products. Complementary information is derived from spectroscopic, often laser-based experiments which determine the internal state distribution of the reaction products. Detailed knowledge of how the available energy in the reactants is channelled into the different degrees of free-

dom among the products will generally give information about the mechanism and the transition state of a particular reaction.

1.1.1 Conceptual Formulation

This work was set out to establish as much information about the dynamics of the gas-liquid interfacial reaction of

$$\mathrm{O}(^3P)\,(g) + \mathrm{C_{30}H_{62}}\,(\ell) \rightarrow \mathrm{Products}\,(g,\,\ell) \tag{1.1}$$

as possible. The foremost aim was to unequivocally establish that the gas-phase molecule OH (or OD for experiments with deuterated squalane, $\mathrm{C_{30}D_{62}}$) is a reaction product. Subsequently, the internal energy distribution, i.e. the vibrational, rotational and fine-structure distribution of the nascent hydroxyl radical, was to be determined. The experiment allowed this to be done at different liquid surface temperatures. Although the experiment was not specifically designed to derive external energy distributions, the kinetic energy distribution and the scattering angle of the hydroxyl radicals with respect to the surface normal were measured with low resolution.

1.1.2 Objectives

Internal energy distributions of the nascent hydroxyl radical were interpreted with the idea to gain information about the mechanism and transition state of reaction 1.1. This task was made easier in the current experiment by the fact that results could be compared with related reactions between $\mathrm{O}(^3P)$ and gas-phase hydrocarbons which have been thoroughly investigated over the past 25 years.[5]
In a more general way, the nature of gas-liquid interfacial reactions was also to be investigated. Whereas homogeneous gas-phase reactions usually occur on the timescale of one single collision (and hence generally show one reaction mechanism only), it is known from reactions at the gas-solid interface[6] and non-reactive scattering experiments on the gas-liquid interface[7] that multiple mechanisms contribute to the overall reaction. In particular, a direct and a trapping-desorption mechanism have usually been detected. In case of the direct mechanism, the reaction seems to occur within a single collision and shows similar characteristics to

gas-phase reactions. In case of the trapping-desorption mechanism, the reaction products seem to remain at the surface for a finite time and exchange energy with the surface. This mechanism is therefore unique to interfacial reactions in that it requires some collision partners in close proximity. Hence it is important in the present experiment to observe any hints whether two mechanisms might also contribute in a gas-liquid interfacial reaction.

Another aim of this project was to gather information about the structure of the liquid squalane surface. Many details are known about the related gas-phase reaction $O(^3P) + C_nH_{2n+2}$, in particular the way the vibrational branching ratio $\frac{OH(v'=1)}{OH(v'=0)}$ changes when $O(^3P)$ reacts with different classes of hydrogen atoms (primary, secondary and tertiary). Therefore another objective was to determine whether any particular hydrocarbon group on the liquid surface is more likely to react with $O(^3P)$ simply by comparison of the internal energy distribution of the title reaction with gas-phase results.

1.2 Motivation

This research is mainly driven by the fundamental question of how the dynamics of gas-liquid interfacial reactions work. However, some links to more applied problems can be made.

Countless reactions take place on the biggest single gas-liquid interface on earth, the sea, every second. Even though energy transfer reactions probably outnumber chemical reactions on the surface of the sea by far, chemical reactions still occur and play a more important role when it comes to reactions on the surface of aerosols just above the surface of the sea. Generally, aerosols both above the sea and above land are found to form micelle-like structures, with their hydrophobic components accumulated at the outer surface of a hydrophilic core, see Fig. 1.1.[8, 9] These aerosols are then inert to uptake of water. Oxidation of the organic compounds at the outside by hydroxyl radicals or, less frequently, $O(^3P)$ atoms convert hydrophobic to hydrophilic components, therefore making the uptake of water much more likely. These aerosols can then act as cloud condensation nuclei and hence have a significant impact on the climate. These processes were the motivation

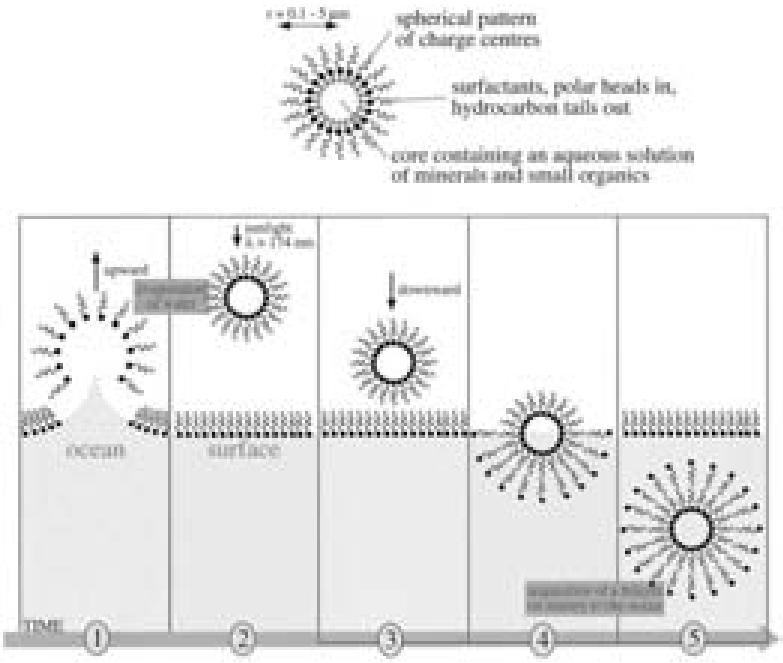

Figure 1.1: Structure and formation of an inverted micelle. The aqueous solution forms the core while the organic components are accumulated at the surface. Adapted from a similar picture in [10].

for kinetic experiments to determine rate constants of reactions between gas-phase species present in the atmosphere and condensed-phase hydrocarbon layers. Naaman and co-workers[11] and Moise and Rudich[12] measured the rate constant between O(^3P) and organised monolayers consisting of saturated hydrocarbon chains. They found that it exceeds the gas-phase rate constant by three orders of magnitude. Similarly, the reaction of OH radicals with a number of hydrocarbon surfaces as investigated by Molina and co-workers[13] shows an increased reactivity over related gas-phase experiments, leading to speculation on the mechanistic reason for the enhancement.

Oxygen plasmas are used in the microelectronics industry to etch (solid) hydrocarbons on circuit boards. Oxygen plasmas are produced by a microwave discharge and contain, apart from oxygen ions and excited oxygen molecules, also oxygen atoms in their ground and excited state.[14, 15, 16] A very similar process, namely the degradation of solid hydrocarbons by O(^3P), represents a very specialised but real concern. O(^3P) is the most abundant species in low-earth orbit (LEO), be-

tween 200 and 700 km above the earth. This is the height where many satellites orbit the earth, and their high velocity as compared to the virtually non-moving $O(^3P)$ atoms results in impact energies up to 5 eV. These collisions initiate the reactions between $O(^3P)$ and the heatshield of the satellite which is usually made of (fluoro)hydrocarbons. The degradation of polymer heatshields was demonstrated by experiments conducted during the flight of the long-duration exposure facility (LDEF). This satellite spent almost six years in low-earth orbit and showed significantly more damaged polymer shields on the leading edge compared to the rear end, an effect mainly attributed to the degradation by $O(^3P)$.[17, 18]

1.3 Previous Experimental Work

This section describes previous related work that formed the motivation and helped in the interpretation of results during this project. Pure dynamical gas-phase experiments as well as the very few experiments carried out on the gas-liquid interface will be described. Very recently, inelastic and reactive scattering experiments on self-assembled monolayers (SAMs) have become popular means to investigate well-ordered surfaces.[19, 20, 21, 22] These systems also represent an interface between experiment and theory as reactions on SAMs can now be simulated using quantum-mechanical methods that would have been reserved for much simpler gas-phase reactions a decade ago.[23, 24]

1.3.1 Experimental Investigations of the Reaction Dynamics of $O(^3P)$ and Gas-phase Hydrocarbons

All relevant experimental studies of the dynamics of the $O(^3P)$ + gas-phase hydrocarbon reaction are described in this subsection. However, an extensive review has been written by Ausfelder and McKendrick recently.[5]

The first experiments to unravel the dynamics of the $O(^3P)$ + hydrocarbon reaction were performed by Andresen and Luntz 25 years ago.[25] These groundbreaking experiments employed cross-molecular beam scattering methods combined with laser-induced fluorescence (LIF) to detect the internal energy distribution of the OH product. Various hydrocarbons were investigated including neopentane

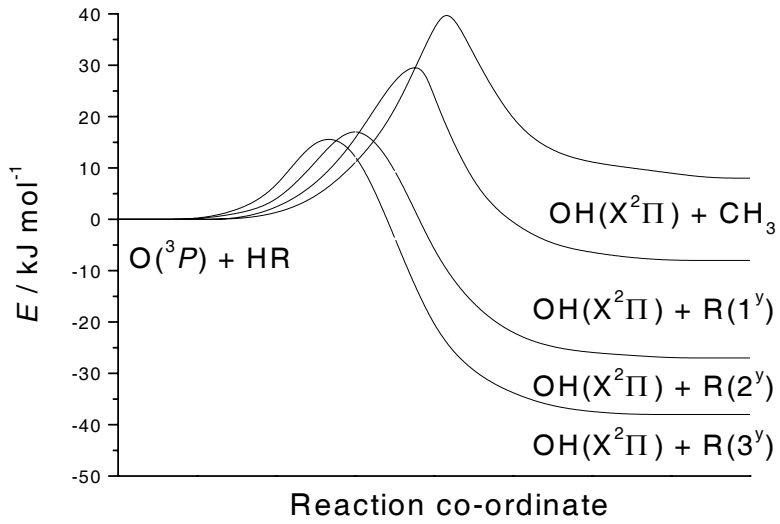

Figure 1.2: Minimum energy paths for the reaction between $O(^3P)$ and saturated hydrocarbons, taken from reference [5].

$C(CH_3)_4$ to probe primary hydrogens, cyclohexane C_6H_{12} for secondary, and isobutane $(CH_3)_3CH$ for tertiary hydrogen atoms. It was shown that the (single) tertiary hydrogen atom in isobutane is far more reactive than the nine remaining primary hydrogen atoms together. As shown in Fig. 1.2, this is due to the activation energy which decreases in the order $\sim$42 kJ mol^{-1} > $\sim$34 kJ mol^{-1} > $\sim$22 kJ mol^{-1} > $\sim$21 kJ mol^{-1} for hydrogen abstraction from methane, primary, secondary and tertiary carbon atoms, respectively.[26] However, the rotational distribution does not seem to vary much for different hydrogen atoms and is found to decline very rapidly with increasing rotational quantum number. This lack of rotational energy was interpreted by Andresen and Luntz as evidence for a collinear transition state in which the C–H–O angle is $\sim 180°$.[25] Such a transition state (shown in Fig. 1.3) would not impart significant torque on the product OH radical.

The vibrational branching ratio $\frac{(v'=1)}{(v'=0)}$ increases from 0.01 for primary hydrogen abstraction to 0.24 for secondary hydrogens to 1.4 for tertiary hydrogens, reflecting the decreasing bond strength.[25]

Whitehead and co-workers improved Luntz' experimental setup by replacing the effusive beam of $O(^3P)$ by a supersonic beam of $O(^3P)$ in He.[27] The main experimental results agreed with the ones by Andresen and Luntz, namely the cold rotational product distribution and the increasing vibrational branching ratio. White-

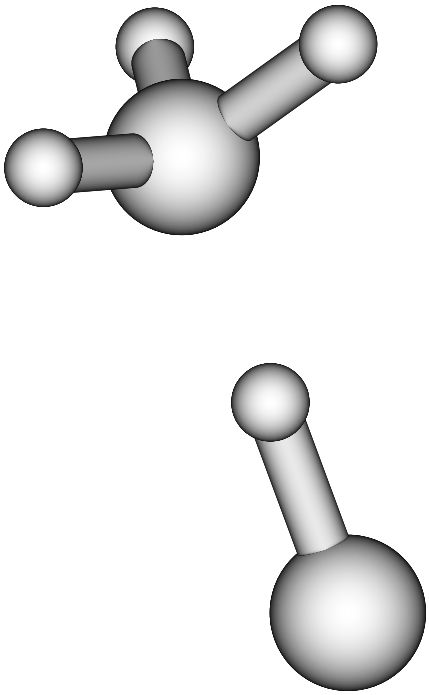

Figure 1.3: Transition state geometry of the reaction $O(^3P) + CH_4$. Bond lengths and angles are very similar to the ones in reference [25].

head and co-workers were then the first to apply the technique of pulsed laser photolysis to the reaction between $O(^3P)$ and saturated hydrocarbons, allowing for improved timing.[28] This method was taken a step further by McKendrick and co-workers who chose a photolysis wavelength for NO_2 just above the threshold for $O(^1D)$ production.[29] Due to the faster kinetic energy distribution, it was therefore possible for the first time to investigate the reaction of $O(^3P)$ with the parent members of hydrocarbons, CH_4 and C_2H_6. No vibrationally excited hydroxyl radicals were observed in these reactions, while the cold rotational state distribution remained unaltered. The reaction of methane and $O(^3P)$ made it also for the first time possible to compare experimental results with more rigorous quantum mechanical calculations as described in subsection 1.4.1.

McKendrick and co-workers also investigated the effects of deuteration in the reaction between $O(^3P)$ and *d*-methane and *d*-cyclohexane.[30] The typical cold rotational product state distribution was confirmed for the reaction with CD_4 and C_6D_{12}. Reaction of $O(^3P)$ with CH_4 does not form any detectable amounts of OH

in $v' = 1$ whereas a very small fraction is formed in the reaction with CD_4, an effect mainly due to the larger reduced mass of the OD radical.

Pirani and co-workers investigated the $O(^3P) + CH_4$ reaction using a molecular beam setup, detecting scattered $O(^3P)$ atoms using mass-spectrometry.[31, 32] They extracted integral cross-sections and managed to map features of the potential energy surfaces.

The first investigation into the stereodynamics of the $O(^3P)$ + gas-phase hydrocarbon reaction was performed by Kajimoto and co-workers using Doppler-resolved polarised laser-induced fluorescence.[33] It was found that the so far assumed backward scattered distribution is only valid at lower collision energies, whereas a forward scattered component becomes more pronounced at higher collision energies. However, this component does not seem to exceed the backward scattered component at collision energies up to $33\,\mathrm{kJ\,mol^{-1}}$.

Suits and co-workers investigated the reaction of $O(^3P)$ with C_6H_{12}, using the velocity map imaging technique to extract the speed and angular distribution of the cyclohexyl radical.[34] They found that the C_6H_{11} radical is mainly backward scattered at collision energies of $24.3\,\mathrm{kJ\,mol^{-1}}$.

A combined experimental and theoretical effort by Garton *et al.* was made to investigate the reaction of $O(^3P)$ and methane, ethane and propane at collision energies as high as $5\,\mathrm{eV}$ ($482\,\mathrm{kJ\,mol^{-1}}$).[35, 36] These studies were motivated by problems occuring in low-earth orbit (LEO) as described in section 1.2. The reaction with short-chain hydrocarbons was intended to model these processes at a level also accessible to theory. In addition to the known abstraction mechanism, an insertion process to form an alcohol intermediate and a C–C bond breakage mechanism were observed at high collision energies. In a similar study by Schatz, Minton and co-workers, the excitation function of the reaction of $O(^3P)$ atoms with methane was investigated, focussing on the reactive product OCH_3.[37]

Very recent work by Liu and co-workers investigated the influence of CH_4 bending excitation in the reaction with $O(^3P)$.[38] It was found that contrary to theoretical predictions vibrational excitation in the bending mode does not enhance the reactivity. Also unexpectedly, excitation of the bending mode produces more vibrationally excited OH/OD rather than umbrella-excited CH_3.

1.3.2 Dynamics of the Reaction between O(^1D) and Gas-phase Hydrocarbons

A large number of groups have investigated the kinetics and dynamics of the reaction between O(^1D) and saturated gas-phase hydrocarbons.[39, 40, 41, 42, 43, 44, 45] O(^1D) atoms are 189.8 kJ mol^{-1} higher in energy than O(^3P) atoms, and rate constants are much faster and the dynamics very different. Whereas a collinear transition state with a C–H–O angle of 180° is generally accepted in the reaction with O(^3P) atoms, two mechanisms seem to dominate the reaction between O(^1D) atoms and gas-phase hydrocarbons.[39] One mechanism is an abstraction mechanism very similar to the one observed in the O(^3P) reaction. The other mechanism involves the insertion of the O(^1D) atom into the C-H bond. The product OH radical is then highly rotationally excited. The ratio between these two mechanisms is mainly determined by the size of the hydrocarbon under investigation with the insertion component being dominant for smaller hydrocarbons.[39, 41]

1.3.3 Reaction Dynamics between O(^3P) Atoms and Liquid Hydrocarbons

Only a limited number of studies have been conducted to investigate the reaction between O(^3P) atoms and liquid hydrocarbons. Hori *et al.* created oxygen atoms by γ-radiolysis of liquid carbon dioxide within the liquid hydrocarbon itself. O(^3P) seemed to be the main oxidising species, but O_2 and O_3 were also formed. Stable products were detected in the liquid phase.[46] Experiments by Zadok and Mazur and by Patiño and co-workers investigated the reaction between gas-phase O(^3P) atoms and liquid hydrocarbons. Oxygen atoms were generated in a plasma above the surface of a liquid hydrocarbon. Again, stable products were recorded in the liquid phase using gas-phase chromatography. The main products in all studies were alcohols or the corresponding ketones.[46, 47, 48, 49] Naaman and co-workers took one step from pure gas-phase experiments to the liquid phase by investigating the reaction between O(^3P) atoms and cyclohexane clusters.[50] Oxygen atoms were formed in a microwave discharge and cyclohexane clusters produced in a molecular beam. Products were detected by laser-induced fluorescence (OH)